

Simulating Local T_g Reporting Layers in Glassy Thin Films

JEFFREY DEFELICE

Department of Chemistry,

Dartmouth College, Hanover, NH 03755

SCOTT T. MILNER

Department of Chemical Engineering,

The Pennsylvania State University, University Park, PA 16802

JANE E. G. LIPSON*

Department of Chemistry,

Dartmouth College, Hanover, NH 03755

Abstract

One of the most notable deviations from bulk fluid properties is the onset of a thickness-dependent glass transition temperature (T_g) for nanometrically thin polymer films. Experimental and theoretical observations suggest that this behavior is a response to the interfaces, which perturb the local properties of a film, and play an increasingly important role in influencing the global properties of a film as its thickness decreases. In this work, we probe the global and local properties of free-standing films using our Limited Mobility (LM) model, which is a simple kinetic lattice model that simulates the dynamics of free volume and mobility in a fluid. We provide insight about the role of mobility in affecting the thickness-dependent film-average T_g of free-standing polymer films by characterizing the depth to which mobility propagates from a free surface, i.e. the “mobile layer depth”. We also consider the effect of “stacking” free-standing polymer films, where confinement by interfaces composed of the same material yields T_g suppression intermediate to that of substrate supported and free-standing films. In order to characterize the local properties of a film, we utilize “reporting layers” located near the free surface and film interior, from which we compute local glass transition temperatures and make connections with experimental results reported for real polymer films.

1. Introduction

Nanometrically thin polymer films have shown some interesting thickness-dependent shifts in a number of properties, relative to that of their corresponding bulk fluid¹⁻⁴. Both experiments⁵⁻²⁰ and theoretical approaches²¹⁻²⁷ provide evidence that the presence of an interface, e.g. a free surface or substrate, causes a perturbation to the physical properties of the region of the film local to it, such as: segmental dynamics,^{5,10,11,24,25} molecular packing efficiency,^{3,6} and the glass transition temperature, T_g ²⁶⁻³⁴. The relative thickness of the perturbed region near an interface grows as the overall film thickness decreases, thus enhancing the influence of local interfacial effects on the global properties of a film,^{3,19,28,31-34} most notable of which is T_g . Depending on the attractive or repulsive nature of substrate-film interactions, which in some cases act in opposition to the local perturbations near a free surface,³¹⁻³⁴ a substrate supported film can exhibit T_g enhancement or suppression relative to that of the bulk. For example, the T_g of a 20 nm thick poly(methylmethacrylate) (PMMA) film supported by silicon oxide is ~ 7 K greater than that of the bulk.^{33,34} On the other hand, the T_g of an equivalently thick silicon oxide supported polystyrene (PS) film is ~ 17 K less than that of the bulk.^{4,19} Another property that may influence T_g enhancement or suppression relative to that of the bulk is tacticity, which has been observed in the case of supported PMMA films.³⁵ Free-standing PS films also exhibit T_g suppression, such that the magnitude of the suppression is notably larger than that of its supported analog; e.g., the T_g of a 20 nm thick free-standing PS film is ~ 70 K lower than that of the bulk.¹⁻³ Indeed, the significant thickness dependence of the film T_g can complicate the use of such films in the field of membrane engineering,^{36,37} where they commonly function to separate gaseous mixtures. Examples include: poly(ethylene oxide) (PEO) which separates CO₂ from N₂,³⁶ polysulfones which separate CO₂ from CH₄,^{36,37} and polyimides³⁷ which separate O₂ from N₂. Such applications underline the importance for providing fundamental physical insight about the influence of free surfaces on the local and average properties of free-standing films.

In this work we apply our Limited Mobility (LM) model^{31,38} to simulate free-standing films for the first time. The LM model is a simple kinetic lattice description of the dynamics of free volume and mobility in a fluid. In our initial application to bulk

systems, we found that the LM model captured features exhibited by a real fluid approaching its glass transition. For example, the length and time scales of static and dynamic heterogeneity diverge according to a power law.³⁸ In subsequent work on supported films we found that the presence of an unbounded source of mobility in the LM model, i.e. a free surface, enhanced the local mobility of a film down to a depth that was temperature-dependent.³¹ One consequence was a thickness-dependent glass transition temperature, analogous to that observed experimentally in polymeric supported thin films.^{1-4,19}

In this work we turn to freestanding films and examine a number of issues related to the presence of free interfaces. We characterize the steady state distribution of mobility across a freestanding film in order to quantify the thickness of the region of enhanced mobility near a free surface, i.e. the “mobile layer depth”. The notion that mobility is enhanced near the free surface is supported by experimental measurements of the mobile layer depth, such as those reported by Ediger and coworkers,⁵⁻⁸ Forrest and coworkers,¹⁰⁻¹² McKenna and coworkers,^{39,40} and others^{13,17,41}. These approaches utilized techniques such as molecular reorientation^{6-8,13} and nanoparticle embedment,^{10-12,17} which directly probe the segmental dynamics by measuring local relaxation times. Among the results reported were that bulk-like relaxation times were not achieved until reaching a film depth that was on the order of 10 nm away from the free surface;^{5-8,10-13,17} This provides an experimental characterization of the mobile layer depth, with which we can make some connections.

We make another connection with experimental results by modeling stacked glassy ultrathin free-standing films in order to probe how the stacking affects T_g . A stacked film comprises hundreds of individual glassy free-standing films, typically 20 – 100 nm thick each, that are assembled without annealing. In results reported by Koh and Simon^{43,44} and others,⁴⁵⁻⁴⁸ the T_g of a stacked ultrathin free-standing film was less than that of the bulk, however, the magnitude of the suppression did not match well with that of an equivalently thick free-standing film. These observations suggest that confinement

of a film between glassified boundaries composed of the same polymeric material can lead to T_g suppression,⁴⁴ a possibility that can be tested in our film simulations.

The LM model allows us to interrogate not only system-averaged effects but also local T_g values, permitting us to probe results for a subset of layers in the sample, which can be chosen as proximate to the free surface or within the interior of the film. This provides the opportunity for direct connection with experimental work by Ellison and Torkelson,¹⁹ in which they characterized the T_g distribution in multilayer films, the existence of which was originally proposed by de Gennes⁴⁹. Fluorescence labeled “reporting layers”, whose intensity was sensitive to local density¹⁹, were located at various depths within a film and used to measure local T_g values in supported,¹⁹ free-standing,²⁸ and bilayer^{15,29,30} films. The results of these measurements provide supporting evidence that there exists a distribution of T_g values across a film, and that the breadth of the distribution provides insight about the length scale over which local mobility is enhanced by a free surface.^{19,28} In the case of free-standing films, they detected a T_g gradient originating from the free surface and extending tens of nanometers into the film.²⁸ Unlike the segmental relaxation time measurements discussed above, a local T_g may be suppressed from that of the bulk over a comparatively longer length scale, thus suggesting a decoupling of segmental dynamics and T_g .⁵ Simultaneous measurements of both local properties, relaxation time and T_g , also provide evidence of decoupling.^{5,50} Yoon and McKenna⁴⁰ and Fakhraai and coworkers⁵¹ have proposed that different experimental techniques, such as those described above, may vary in their sensitivity to a film’s T_g . Indeed, this may be an extension of similar behavior that has been observed in the bulk case.⁵²⁻⁵⁴

Recent reviews by Priestly et al.⁵⁰ and Ediger and Forrest⁵ have raised the issue of the differences in dynamic versus thermodynamic routes to local T_g determination, as a means of characterizing the thickness of the region of enhanced mobility. Their analyses highlight the need for further experimental and theoretical insight that focuses on the distribution of local properties within a film, particularly near the glass transition. Our LM model is well suited for such a study, since we are able to calculate the long-time

average mobility of selected regions, i.e. “reporting layers”, and thus able to characterize the variation in properties (such as a local T_g) across freestanding films of varying total thicknesses. Here we should note that our films are “pure”, in the sense that they do not contain any dispersed foreign particles, in contrast to some of the experimental studies^{10-12,17,29}. It is also important to note that, while the LM approach incorporates effects of local cooperativity (as described in the next section, associated with rules regarding translation of mobility), it does not model effects of chemical connectivity, given that whatever material may occupy one of the lattice sites is not “bonded” in any way to adjacent sites.

The paper is organized as follows: We begin with a brief overview of the LM model in Section 2. In Section 3, we characterize the thickness of the region of enhanced mobility near a free surface and how it is controlled by the LM model parameters. We then examine the distribution of mobility across a free-standing film and its connection with T_g in Section 4. Sub-sections 4a and 4b focus on the film-average T_g of free-standing films and stacked free-standing films, respectively. In Section 5 we turn to local film properties, where we probe the local T_g of free surface “reporting layers”, which consist of the layers of a film near a free surface. Section 6 covers the local T_g of reporting layers located at the film interior. These reporting layers are located away from the surface, and are “sandwiched” by surrounding film layers. In each section connections are made to available experimental results. Finally, in Section 8, we summarize our discussion and draw conclusions.

2. Limited mobility model

The following is a brief description of the Limited Mobility (LM) model, used in this work to simulate free-standing films for the first time. Previous applications of the LM model include: bulk, buried slab, and substrate supported film systems,^{31,38} to which we direct the reader for additional information.

The LM model is a two-dimensional kinetic lattice model, where each lattice site represents a fluid element in one of three possible states: “mobile”, “dormant”, or

“dense”. The states correspond to three possible designations of relative mobility, as suggested by fluid simulations^{55,56}: mobile, dormant, and dense, respectively. A ‘mobile’ site represents a localized “active” region within a fluid, associated with either local diffusion, via “string-like” motion,⁵⁶ or spontaneous relaxation such that mobility is locally dispersed⁵⁵. The latter situation results in a site being considered ‘dormant’. A dormant site can evolve to become mobile; however, it cannot happen independently. Instead, neighboring mobility is required in order to assist, which means that transition of a site from being dormant to being mobile must be facilitated; this can occur when a nearest-neighbor is, itself, a mobile site.

The LM model is initialized by randomly assigning mobile, dormant, and dense sites to positions on a square lattice. We consider each lattice site to have eight neighbors: four nearest and four next-nearest. The initial fractions of mobile, dormant, and dense sites are chosen and this results in initial values for the fraction of free volume, ϕ , which is the sum of dormant and mobile site fractions, and the fraction of the free volume that is initially mobile, ψ . As the simulation runs, the site fractions evolve toward steady state values for ϕ and ψ that depend on the parameter choices (discussed below), independent of the initial conditions. As we have done in previous work,^{31,38} here we initialize our systems with random configurations such that $\phi = 0.4$ and $\psi = 0.5$. The system evolves via Monte Carlo dynamics by attempting an operation on a randomly selected lattice site, such that one system sweep represents a number of attempted operations that is equal to the total number of lattice sites. Every system is equilibrated for 5×10^5 system sweeps, followed by an additional 5×10^5 sweeps over which statistics are collected. The attempt probability of each type of operation is 1/3, regardless of the identity of the randomly selected lattice site. The types of operations are illustrated in Figure 1, and are described further below.

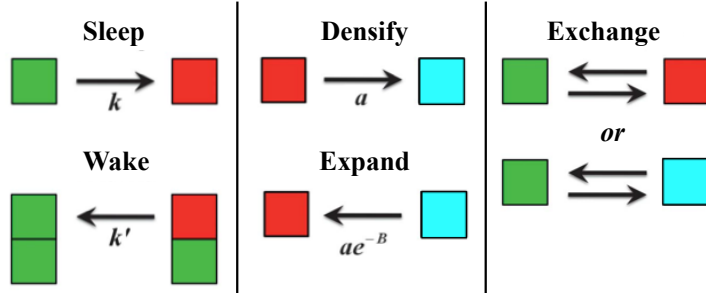


Figure 1: Illustration of the Limited Mobility model Monte Carlo moves, shown with corresponding attempt probabilities. Green, red, and blue squares represent “mobile”, “dormant”, and “dense” lattice sites, respectively.

- *Sleep* and *wake*: a mobile site may become dormant (“sleep”) with probability, k . The reverse of this operation, i.e. a dormant site becoming mobile (“wake”), may occur with probability k' , and must be *facilitated* by at least one adjacent mobile site.
- *Densify* and *expand*: a dormant site may become dense (“densify”) with probability, a . The reverse of this operation, a dense site becoming dormant (“expand”), may occur with a probability ae^{-B} . The parameter B reflects the strength of an external field imposed on the system, which controls the fraction of dense sites. We interpret the parameter B as an inverse temperature, analogous to the external field in the Fredrickson-Anderson kinetically constrained Ising model⁵⁷.
- *Exchange*: a mobile site may swap positions (“exchange”) with a randomly selected neighboring site of any type, i.e. dormant, dense, or mobile, with probability 1. A dormant or dense site may swap with a randomly selected neighbor *only if that neighbor is mobile*, also with a probability of unity.

The system evolves via the dynamic operations described above, eventually reaching steady state fractions of mobile, dormant, and dense sites. We can thus compute the long-time average fractions of total free volume and mobile free volume, $\bar{\phi}$ and $\bar{\psi}$, respectively. The single critical point of the LM model occurs in the bulk when the steady state fraction of mobile free volume reaches zero ($\bar{\psi} = 0$). On one side of this critical point, the system maintains a finite fraction of mobile sites, which exhibit static and dynamic heterogeneity reported in previous work³⁸. Beyond the critical point, only

dormant free volume and dense sites persist, thus the system is “kinetically arrested”. Once the system is arrested, it is impossible for a site to spontaneously become mobile.

The independent parameters k , k' , and B control the state of the system, i.e. whether it is above or below kinetic arrest. We have shown³¹ that the critical point of the LM model can be reached by fixing any two of the parameters (k, k', B) , while varying the third. For example, one may fix the parameters k and k' , and vary B . Recall that the parameter B is analogous to an inverse temperature, $B \propto 1/T$, so from this point forward our discussion will be in terms of T . The average fraction of total free volume in the LM model, $\bar{\phi}$, changes with T , analogous to the response of a real fluid due to a change in temperature. Thus we interpret that the variable $\bar{\phi}$ is inversely proportional to density, i.e. large $\bar{\phi}$ implies low density, and vice versa. Above the bulk kinetic arrest temperature, T_a , the long-time average fraction of free volume satisfies the self-consistent expression:

$$\bar{\phi} = \frac{e^{-1/T} + \bar{\phi}\bar{\psi}}{1 + e^{-1/T}} \quad (1)$$

In the absence of mobile sites ($\bar{\psi} = 0$), the critical density, ϕ^* , can be computed analytically by:

$$\phi^* = \frac{e^{-1/T}}{1 + e^{-1/T}} \quad (2)$$

Note that the relationships expressed in Equations 1 and 2 are independent of the parameter a , which is a factor in both the densify and expand attempt probabilities. The magnitude of the kinetic arrest temperature, and thus ϕ^* , depends on the choice of k and k' .³¹ Recently, however, we have shown that ϕ^* is essentially unaffected by a change in the individual values of k and k' on the condition that the ratio k/k' remains constant.⁵⁸ In the following section we provide new insight about how k/k' controls the depth to which mobility propagates into a film from a free surface.

Turning to simulations of free-standing films, which is the focus of this work, we must account for the two free surface boundaries. In the LM model, each free surface is represented by a single lattice layer of permanently mobile sites. One free surface is always located at lattice layer $z = 0$, where the z -dimension is perpendicular to the free surface (and is measured in lattice units). The location of the other free surface, at a finite value of z , specifies the film thickness, h . The lattice is periodic in the direction parallel to the free surfaces, and the number of lattice sites in this direction was fixed to be 100 in this work. The free surface boundary conditions for the LM model are illustrated in Figure 2, and described further below.

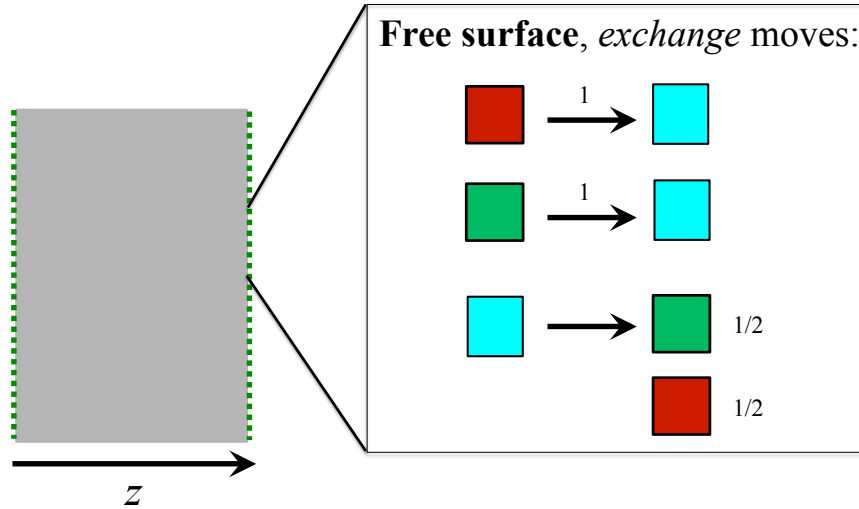


Figure 2: Illustration of Limited Mobility model “exchange” moves imposed upon lattice sites located at a free surface of a film system.

A free surface can act as either a source or sink of mobility upon an attempted exchange operation by a lattice site in the directly adjacent layer. If a dormant or mobile site in the layer adjacent to the free surface (e.g., a site located at $z = 1$) attempts to exchange with a site in a free surface layer (e.g., $z = 0$), then that site becomes dense with probability 1. On the other hand, if a dense site attempts this operation, then it becomes either mobile or dormant, each with probability of 1/2. Therefore, the chemical potential for adding or subtracting mobile sites at a free surface is zero, independent of the model temperature, thus a free surface acts as an *unbounded* source and sink of mobility. It is for this reason that unlike the bulk, a film will not reach kinetic arrest (except at zero temperature), and

thus there is no temperature at which mobility will completely disappear. Instead, we define a “glassy” cut-off in the average mobility, $\bar{\psi} = 0.10$, which is approximately $1/z$, the reciprocal of the number of neighbors per lattice site. The glass transition temperature of a film or the bulk, T_g , is the temperature at which the average mobility $\bar{\psi} = 0.10$. This definition of glassiness was used in previous work on supported films³¹ and in earlier lattice model approaches to the glass transition⁵⁹.

3. Mobile layer depth

The thickness of the region of enhanced mobility near a free surface, which we term the “mobile layer depth”, is of particular interest. It has been suggested that the relative contribution from the mobile layer to the total film T_g increases as the overall film thickness decreases, thus leading to the thickness-dependent T_g suppression reported for free-standing films^{3,28}. Our model is particularly suited for characterizing the steady state distribution of mobility across a film, which puts us in the position to make connections with two categories of experimental results.

In the first category, Paeng et al.⁶⁻⁸ have characterized the length scale over which the local dynamics of a film are enhanced by a free surface using measurements of fluorescent probe anisotropy. Another contribution to this category involves nanoparticle embedment, as in the work of Qi et al.^{10,11}, Fakhraai and Forrest,¹² and McKenna and coworkers^{39,40}. All of these results, which probe local dynamics, suggest that there exists a 2 – 10 nm thick region near the free surface of a film where the local relaxation is enhanced relative to that of the bulk. Some of the results indicate that the mobile layer thickness exhibits a dependence on chemical structure,⁶ which we will discuss in more detail below. In all reported cases, however, bulk-like relaxation times were observed beyond a film depth of 10 nm.

In a second category are experimental results from Torkelson and coworkers^{19,28} and Roth and coworkers^{20,29,30}. These researches measure the shift in fluorescence intensity of a labeled layer located near the free surface of a film, from which they characterize the local T_g . Unlike the (dynamic) local relaxation time measurements

described above, these measurements are sensitive to the local density.¹⁹ The local T_g measurements indicate that there exists a T_g gradient that extends several tens of nanometers into a film from a free surface, thus suggesting a longer length-scale than 10 nm over which the local dynamics are enhanced by a free surface.

The LM approach characterizes the steady state distribution of mobility throughout a free-standing film, and the local T_g values as a function of position throughout a film. Given how we quantify mobility, this leaves us in a position to make a more direct comparison with the experimental techniques that reflect measurements of density. However, we are also interested in the dynamic studies to the extent that they help us to illuminate trends.

Here we provide an analysis of the mobile layer depth using the LM model, and describe how the parameters k and k' control it. We have chosen to define the mobile layer depth in the LM model³¹ as the layer, z , at which $\bar{\psi}(z) = 0.05$. This value is slightly less than the glassy cut-off of $\bar{\psi} = 0.10$, in recognition that some mobility persists below T_g . Next, we are interested in the combination of k and k' that optimize the propagation of mobility from a free surface into a film. These parameters, which represent the “sleep” and “wake-up” move attempt probabilities, respectively, reflect intrinsic temperature-independent characteristics of the system.^{31,38,58}

We have shown in recent work⁵⁸ that for a fixed value of the ratio k/k' the bulk T_g does not vary significantly when the individual values of k and k' are increased by a factor of two. Thus, it is useful for the purpose of comparison to combine the parameters k and k' such that we may consider how mobile layer depth varies with respect to the ratio k/k' . However, T_g does vary with the value of the ratio k/k' : a bulk fluid with large k/k' reaches T_g at a higher temperature than that with a smaller k/k' .^{31,58} In the case of a film, we are limited in our choice of k/k' if we want our system to exhibit a glass transition. For example, reducing the ratio k/k' raises the film-average mobility such that even at low temperatures $\bar{\psi} > 0.10$. This means that for sufficiently low k/k' it would be impossible to glassify the system. Conversely, in the limit of large k/k' the film-average

mobility is diminished to the extent that even at infinite temperature ($1/T = 0$) the system exhibits $\bar{\psi} < 0.10$, which also precludes the existence of a T_g . Thus we begin by considering the change in mobile layer depth as a film is cooled below its bulk T_g for a limited, but feasible, range of choices of k/k' . Some results are summarized in Figure 3.

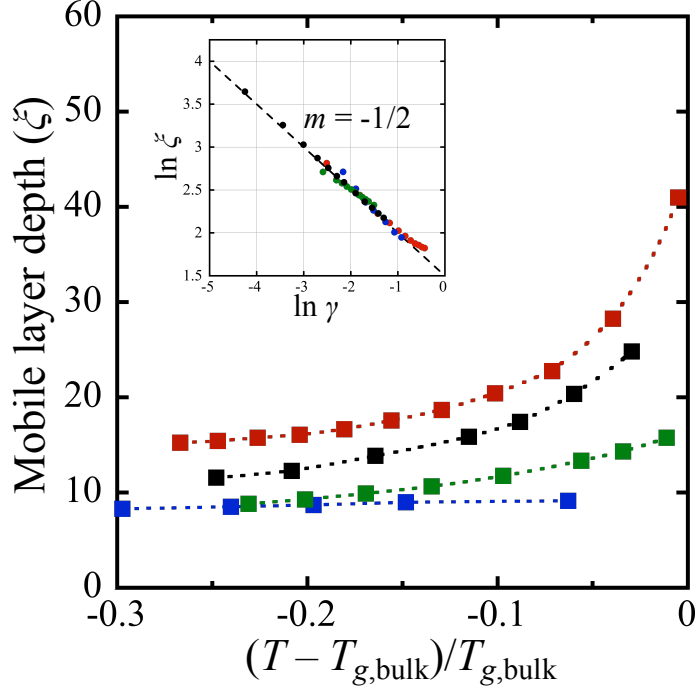


Figure 3: Mobile layer depth, ξ , for a series of films cooled to temperatures below their corresponding bulk glass transition temperature, plotted as the quantity $(T - T_{g,\text{bulk}})/T_{g,\text{bulk}}$. Data sets correspond to films with $k/k' = 0.33$ (red), 1.00 (black), 1.33 (green), and 2.33 (blue). Dashed lines are guides to the eye. The inset log-log plot shows the scaling of ξ with the critical parameter $\gamma = (\phi^* - \phi)/\phi^*$; the dashed line has a slope $m = -1/2$.

For each ratio of k/k' the mobile layer depth, ξ , decreases as a film is cooled below its bulk T_g . We also observe that the extent to which mobility penetrates into a film at a given distance from T_g depends on the ratio k/k' . As k/k' increases from a value of 0.33 (red) to 2.33 (blue) the “wake-up” move becomes increasingly unlikely relative to the “sleep” move; the result is shallower mobile layer depths. For example, when $(T - T_{g,\text{bulk}})/T_{g,\text{bulk}} = -0.1$, the mobile layer depth $\xi \approx 20$ for $k/k' = 0.33$ whereas $\xi \approx 10$ for $k/k' = 2.33$. Thus by increasing the ratio of k/k' we can inhibit the propagation of

mobility from a free surface into a film. Indeed, increasing the ratio k/k' beyond the values shown here would yield mobile layer depths that approach $\xi = 0$.

The LM model relationship between the mobile layer depth and the value of k/k' , illustrated in Figure 3, appears to be analogous to the dependence of the mobile layer depth on chemical structure reported by Paeng and Ediger⁶ (see Figure 5 in ref. 6). Here we briefly summarize their observations in order to make a connection with our own results. Paeng and Ediger utilized measurements of the molecular reorientation of a fluorescent probe to determine the mobile layer depths of five chemically distinct polymer films [poly(2-vinylpyridine) (P2VP), PS, PMMA, poly(4-*tert*-butylstyrene) (PtBS), and poly(α -methylstyrene) (P α MS)]. The mobile layer depths for these polymers at their corresponding bulk T_g values ranged from 0 – 10 nm. For example, the mobile layer depth of PtBS was approximately equal to 10 nm while that of P α MS was approximately equal to 0 nm. The authors reported that no clear correlations emerged between the thicknesses of the mobile layers and a number of physical properties, including: bulk T_g , fragility, Kuhn length, or the length scale of cooperatively rearranging regions (CRRs), for this set of polymers⁶. Instead, they rationalized the variability of the mobile layer depths in terms of the amplitude of the surface perturbation, suggesting that the system specificity may be related to molecular packing efficiency near a free surface.

Turning to the results shown in Figure 3, we find in the LM model that increasing the ratio k/k' decreases the mobile layer depth. This appears to be analogous to experimental trends which show the effect of changing the chemical nature of the molecules comprising a real film,⁶ and suggests that the ratio k/k' may effectively serve to characterize some intrinsic property of a real fluid. Here it is important that we reiterate the limit of our ability to compare with such data. Our characterization of the mobile layer depth reflects the region in which the *long-time average* fraction of mobile sites is locally enhanced. Paeng and Ediger's measurements lead them to estimate the mobile layer thickness, through locally enhanced *dynamics*⁶. Relative to their results we observe some of the same trends: The mobile layer thickness increases monotonically

with temperature, and chemically distinct samples (denoted in our case by different values of k/k') are distinguishable in their behavior.

The inset of Figure 3 illustrates the scaling behavior of $\ln\xi$ with $\ln\gamma$ for all choices of k/k' , where $\gamma = (\phi^* - \phi)/\phi$, and ϕ^* is the density at the bulk kinetic arrest transition. The two sets of results in the figure show that although the *value* of the mobile layer depth, ξ , at a given distance from the glass transition can be controlled to some extent by varying k/k' , the manner in which mobility grows with temperature obeys a ‘universal’ scaling relationship, $\xi \propto \gamma^{-1/2}$, regardless of the choice of k/k' .³¹

In this work, we will proceed with the choice $k/k' = 1$ (black data set in Figure 3), which yields moderate propagation of mobility into the film interior and where the film-average mobility reaches the $\bar{\psi} = 0.10$ cutoff at a finite value of T . Note that the choice of $k/k' = 1$ (i.e. exactly equal to unity) is for convenience; picking any number with the same order of magnitude, in either direction, would work equally well. Having chosen the ratio to be fixed, in Figure 4 we illustrate that changing the individual parameters k and k' , while maintaining the ratio, also has an effect on the mobile layer depth.

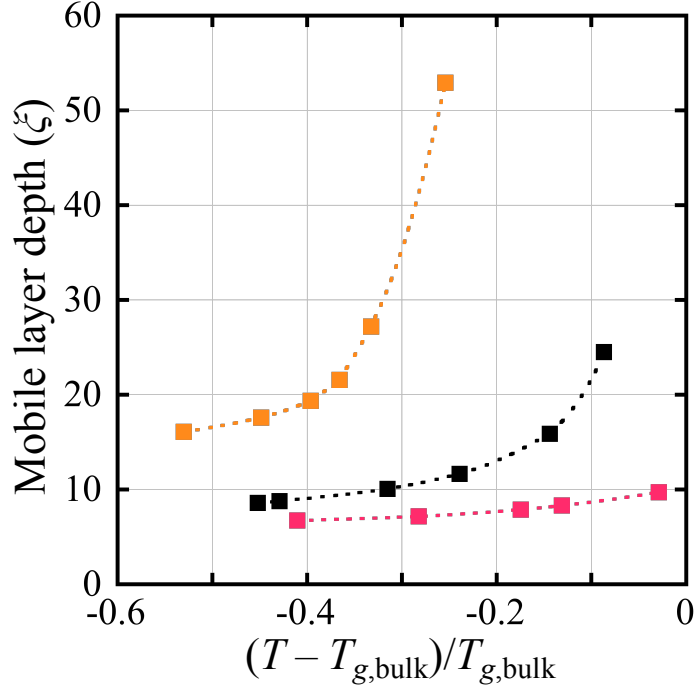


Figure 4: Mobile layer depth, ξ , for a series of films cooled to temperatures below their corresponding bulk glass transition temperature, plotted as the quantity $(T - T_{g,\text{bulk}})/T_{g,\text{bulk}}$. Data sets correspond to films where $k = k' = 0.10$ (orange), 0.40 (black), and 0.70 (pink), such that in all cases $k/k' = 1$. Dashed lines are guides to the eye.

In each data set the individual values of k and k' increase from 0.10 (orange) to 0.70 (pink) while the ratio $k/k' = 1$ is fixed. At any temperature below their respective T_g values, we observe the greatest mobile layer depths for $k = k' = 0.10$. Thus we can further optimize the propagation of mobility into a film for the choice of $k/k' = 1$ by reducing the individual values of k and k' . This feature allows us to probe the local T_g of a “sandwiched” reporting layer located at the center of a film since, if mobility fails to propagate relatively deep into a film, we would be severely limited in the range of film thicknesses for which we would observe a shift in T_g from that of the bulk. This is discussed in greater detail in Section 6.

4. Free-standing film mobility

We now turn to the steady state distribution of mobility throughout a free-standing film. In Figure 5a, we show profiles representing the average fraction of mobility at each layer, $\bar{\psi}(z)$, as a function of film depth, z , for a 40 layer free-standing

film (with $k = k' = 0.4$). The results correspond to two different model temperatures: $T = 1.00$ (red points), which is above the bulk $T_g = 0.73$, and $T = 0.50$ (blue points), which is below the bulk T_g .

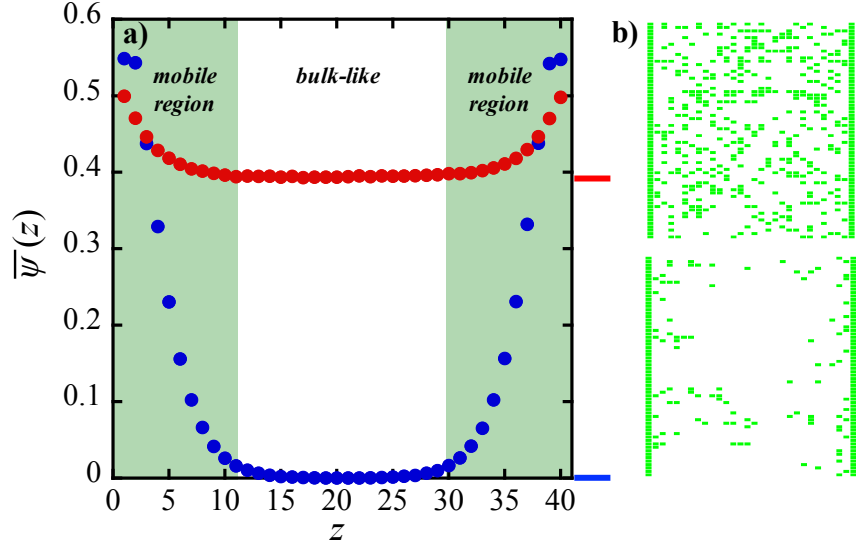


Figure 5: (a) Average mobile fraction of free volume, $\bar{\psi}(z)$, at each layer, z , of a free standing film ($k = k' = 0.4$) above ($T = 1.00$; red points) and below ($T = 0.50$; blue points) the bulk glass transition temperature, $T_g = 0.73$. Solid horizontal lines at right of (a) are $\bar{\psi}$ values of analogous bulk systems with simulation parameters matching those of their correspond film simulations. (b) Simulation snapshots of mobile sites, corresponding to the results shown in (a): top – above bulk T_g , bottom – below bulk T_g .

Above the bulk T_g , there is slightly enhanced mobility in the layers that are local to either free surface (layers 1 – 10 and 30 – 40). The average mobility of layers 1 – 10 and 30 – 40 decays as $\sim z^{-0.1}$ with respect to the free surface. The average mobility between layers 10 – 30 is constant and equal to that of the bulk at the equivalent temperature. Therefore, the enhancement of mobility, which originates from either of the free surfaces, extends to a finite depth within the film; i.e., there exists a gradient of mobility. The mobility gradient increases as a free-standing film is cooled below its bulk T_g . Under these conditions, the average mobility of the layers local to the free surfaces (layers 1 – 14 and 26 – 40) is significantly enhanced relative to that of the film interior (layers 14 – 26), where essentially no mobility is present. The average mobility of layers 1 – 14 and 26 – 40 decays exponentially, as $\sim e^{-0.4z}$ with respect to the free surface. Further illustration of

this behavior is provided in Figure 5b, where we show simulation snapshots of mobile sites *only* (the white region includes both dormant and dense sites). The top and bottom snapshots correspond to the film at temperatures above and below the bulk T_g , respectively. Note that that the solid green layers of mobile sites represent the free surfaces that confine the film. Above the bulk T_g , mobility is distributed almost homogeneously throughout the film, whereas below the bulk T_g it is localized to only the regions near the free surfaces. In the latter case the mobile sites within the film are not only sparse, they are also heterogeneously distributed, a finding that parallels our characterization of how glassy regions grow in a bulk sample^{31,38}.

As we have shown in Figure 5, approximately 20 layers of a 40 layer-thick free-standing film exhibit enhanced mobility relative to the film interior at a temperature well below the bulk T_g . Thus the sample average, or equivalently, the film-average mobility is greater than that of a bulk sample at the same temperature. However, the depth to which mobility propagates into a film from a free surface is *independent* of the total film thickness.³¹ Therefore, as a film gets thinner the interior region of the film represents a smaller fraction of the overall contribution and the film-average mobility increases. The next portion of this section focuses on the film-average glass transition temperature in the LM model, which is related to the film-average mobility. Sections 5 and 6 will address local behavior.

4a. Free-standing versus supported films

Recall that the glass transition temperature for a film in the LM model, T_g , is defined as the temperature at which the long-time average mobility $\bar{\psi} = 0.1$. In Figure 6, we show the deviation of a film's glass transition temperature from that of the analogous bulk sample, $\Delta T_g = T_g - T_{g,\text{bulk}}$, as a function of film thickness, h (in lattice layers), for free-standing, substrate supported, and stacked free-standing films. [Note that the temperature scale is internal to the model (see Section 2 for further detail), and does not directly map to experimental temperature]. In the previous section, we described the free surface boundary conditions for a free-standing film. Note that the model conditions for the single free surface boundary of a substrate supported film are identical. The substrate

boundary, however, consists of a lattice layer of permanently “dense” sites, which do not interact with sites in the adjacent layer; e.g., an attempted exchange operation by a site in the adjacent layer with a site on the substrate will fail.³¹ The boundary conditions and results of our stacked free-standing film simulations will be described in the next section.

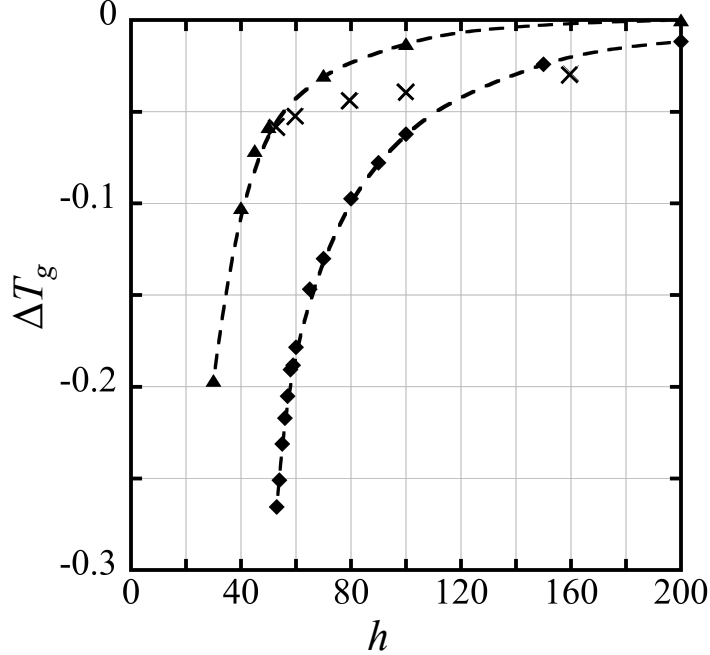


Figure 6: Deviation in film-average glass transition temperature from the bulk, $\Delta T_g = T_g - T_{g,\text{bulk}}$, for films of thickness h (in lattice units) with $k = k' = 0.4$; substrate supported (triangles), free-standing (diamonds), and stacked (crosses). Dashed lines are guides to the eye.

As shown by the results for substrate supported (triangles) and freestanding (diamonds) films in Figure 6, the LM model predicts suppression of the glass transition temperature relative to that of the bulk as film thickness decreases. This behavior is consistent with the stronger of the two transitions, viz. the upper transition, reported by Pye and Roth,⁶⁰ which they concluded was molecular-weight-independent, as are our own results. In both cases, the region(s) of enhanced mobility near the free surface(s) represent a greater fraction of the overall film’s thickness as the net film thickness decreases. This raises the film-average mobility, requiring greater cooling in order to reach a glassy state. In contrast to the free-standing case, however, one of the substrate supported film boundaries is a non-interacting dense layer. In the layers local to the substrate boundary,

mobility is slightly suppressed.³¹ Therefore, at a temperature T , the film-average mobility of a free-standing film will always be greater than that of a substrate supported film of equivalent thickness. Consequently, a freestanding film of thickness h requires a lower temperature to glassify than a substrate supported film of thickness h . Indeed, the presence of a second free surface approximately doubles the extent of T_g suppression, relative to that predicted for a substrate supported film. The LM model predictions are therefore consistent with experimental studies, where it has been reported that the magnitude of ΔT_g for a polystyrene (PS) free-standing film of thickness h is equivalent to that of a silicon substrate supported PS film of thickness $h/2$.⁶¹

Although our simulations were not intended to map to the behavior of a specific polymer, e.g. a PS film, we find that the relevant range of thicknesses over which our film T_g values are suppressed from that of the bulk, shows an internal consistency that matches well with experiment. In particular, the results of time-independent experimental techniques that are sensitive to density, such as: ellipsometry^{1,4,9,18,62} and fluorescence intensity^{2,19,20,28-30}. For example, the T_g values reported for a 20 nm thick silicon oxide-supported PS film¹⁹ ($T_g = 356$ K) and a 30 nm gold-supported PMMA film⁴ ($T_g = 382$ K) are the most suppressed from their corresponding bulk values, which are 373 K and 390 K, respectively. For both PS and PMMA, supported films greater than 100 nm in thickness yielded a bulk-like T_g .^{4,19} Our simulations indicate analogous behavior over a thickness range of 30 – 120 layers for supported films; in both cases, bulk behavior is observed for a thickness about fourfold larger than that exhibiting the greatest suppression. This provides a way to translate the relevant film thickness range of our film simulations to that of experimental measurements, and leads us to conclude that 1 lattice layer corresponds to roughly 1 – 2 nm for these systems.

In addition, we can consider the connection between changes in T_g as reflected in our model temperature scale with experimental measurements of changes in T_g . Although the LM temperature scale is internal to the model, we find that the shift in T_g values relative to $T_{g,\text{bulk}}$ compares reasonably well with experiment. For supported films, experimental measurements¹⁹ of $\Delta T_g/T_{g,\text{bulk}}$ range in value from 0 to approximately -0.10

as the film thickness of silicon oxide-supported PS decreases below \sim 100 nm. Our results for substrate supported films range in value from 0 to -0.27 as film thickness decreases below 120 layers. For free-standing films, experimental measurements of $\Delta T_g/T_{g,\text{bulk}}$ range in value from 0 to approximately -0.20 for PS³ and 0 to approximately -0.30 for polycarbonate,^{63,64} as film thickness decreases below \sim 100 nm. Our results for free-standing films range in value from 0 to -0.37 over the relevant film thickness range.

4b. Stacked free-standing films

Using the LM model, we can control boundary conditions; e.g., control the flow of mobility. This lead us to be interested in experimental results on systems where the nature of the boundaries changed over the course of the experiment, namely, results from Koh and Simon^{43,44} and others,⁴⁵⁻⁴⁸ in which a set of ultrathin free-standing films were prepared below their T_g and then combined to give an overall thickness comparable to a bulk sample. The stack was then heated using a differential scanning calorimeter (DSC) in order to record the glass transition temperature. While isolated \sim 20 nm PS³ and \sim 15 nm PMMA films⁶² (i.e., individual freestanding films) showed T_g suppression of -70 K and -30 K, respectively, stacking yielded T_g suppression comparable to what similarly thick substrate-supported films exhibited: -8 K for stacked PS⁴³ and -10 K for stacked PMMA⁴⁵. In a third case, the T_g values of stacked poly(2-chlorostyrene) (P2CS) films were found to be intermediate to those of its substrate supported and free-standing equivalents⁴⁶. For all three polymers, annealing the stacked films, which facilitated interpenetration of the polymer chains, yielded a sample which exhibited the bulk T_g .^{43,45,46}

Using the LM model we constructed one slice of a film stack by first simulating a free-standing film that had reached its steady state at a temperature below its glass transition temperature, i.e. $T < T_g$. In order to best approximate what the experimental setup might represent, we then replaced the free surface boundaries, which are made up of permanently mobile sites, by the steady-state composition of the adjacent lattice layers. That is, the free surface boundary at lattice layer $z = 0$, was replaced with a *copy* of the configuration of layer $z = 1$, which would comprise a mixture of mobile, dormant, and

dense sites. As always, in heating this film in order to determine its glass transition temperature we kept the compositions of the two boundary layers (at $z = 0$ and $z = h$) fixed. This meant that no exchanges of mobility could occur between a boundary and its adjacent layer, and thus the boundary in this case would no longer act as a source/sink of mobility (unlike the completely free surface). However, the mobile sites present in the boundary layer, which comprised less than 20% of the boundary sites, could still serve to facilitate a “wake up” move attempted by a dormant site in the adjacent layer.

The results of our stacked film simulations are shown as crosses in Figure 6. The LM model predicts that a stacked film also exhibits a T_g reduction relative to the bulk, the value of which falls roughly between those of substrate supported and free-standing films. The positioning of the stacked film results between those for the supported and the free-standing films is consistent with what was found experimentally for the stacked film systems, which were described above. These results support the interpretation of stacked confinement as representing a film environment intermediate between that of a free-standing film and that of a substrate supported film. Here we note that the stacked film results shown in Figure 6 correspond to simulations of individual slices of a stacked film. However, since no exchanges of mobility would be able to occur between slices the composition of each stacked film slice would evolve independently of its neighboring slices. This situation is analogous to the experimental setup involving a stack of films that have not been annealed.

Further, we find that “annealing” our stacked films yields the bulk T_g , which is also consistent with the experimental results summarized. In order to simulate annealing using the LM model, a stacked film was heated above its T_g such that at $T > T_g$ the stacked boundary layer conditions were removed, thus permitting mobility (green sites) to translate across the boundary. This mimics the effect of annealing a real stacked film, which allows for inter-diffusion of the polymer chains between stacked layers⁴³. Following equilibration at $T > T_g$, the film was cooled from the melt to determine its T_g , and we found that the T_g of an annealed stacked film was equal to the bulk value.

Therefore, in both our simulations of stacked films and measurements of real stacked films, annealing reverses the effect of the stacked confinement on T_g .

5. Free surface reporting layers

In the previous section, we observed that enhanced mobility in the layers local to a free surface increasingly perturbs the film-average mobility as film thickness decreases. As a result, the extent to which the film-average glass transition temperature is suppressed relative to the bulk, ΔT_g , grows as film thickness decreases. In this section we focus on the local mobility of those layers near a free surface, and probe the local glass transition temperature of this region.

Recent experimental work, notably that of Roth and coworkers^{20,29,30} and Torkelson and coworkers,^{19,28} has utilized fluorescence labeling to characterize not only the overall film-averaged T_g , but also the T_g of a slice of the film, positioned at different depths within the film, for substrate supported, free-standing, and bilayer films. For example, a pyrene-labeled layer of PS, typically \sim 10-15 nanometers in thickness, has been embedded at various depths within a neat-PS film^{19,28}. The pyrene-labeled layer, which is fluorescence active, acts as a “reporting” layer for the local density and thus a measure of the local T_g . For free-standing PS films, Kim and Torkelson²⁸ reported on the T_g of a 14 nm reporting layer located at the free surface of a film, for overall film thicknesses ranging from 50 – 100 nm. They observed that the T_g of the free surface reporting layers was constant, i.e. independent of total film thickness, and suppressed from that of the bulk such that $\Delta T_g = -34$ K. On the other hand, for freestanding films having overall film thicknesses less than 50 nm, the surface layer shift in T_g became more pronounced as the film thickness decreased. They concluded that below some characteristic overall thickness the free surface reporting layers near one of the surfaces are also perturbed by the presence of the other free surface.²⁸

With the LM model we can easily determine the long-time average mobility of layers near a free surface in freestanding films via an approach analogous to that of the experiments described above. We simulated a set of films of varying total thickness and

computed the average mobility over the 30 lattice layers nearest to the free surface. This region of fixed thickness represents our “reporting layers”. Two key factors were weighed in the selection of the reporting layer thickness: 1) it should be sufficiently thin so as to represent behavior local to the free surface, and 2) it must be sufficiently thick so as to reach the glassy cutoff in mobility that we have defined above. In terms of the latter, recall that the T_g of the free surface reporting layers is the temperature at which the long-time average mobility over the reporting layers reaches the cutoff $\bar{\psi} = 0.10$.

In Figure 7, we show the deviation of the free surface reporting layers’ glass transition temperature from that of the analogous bulk sample, ΔT_g , as a function of the overall film thickness, h . We have also included the free-standing whole film-average results for reference.

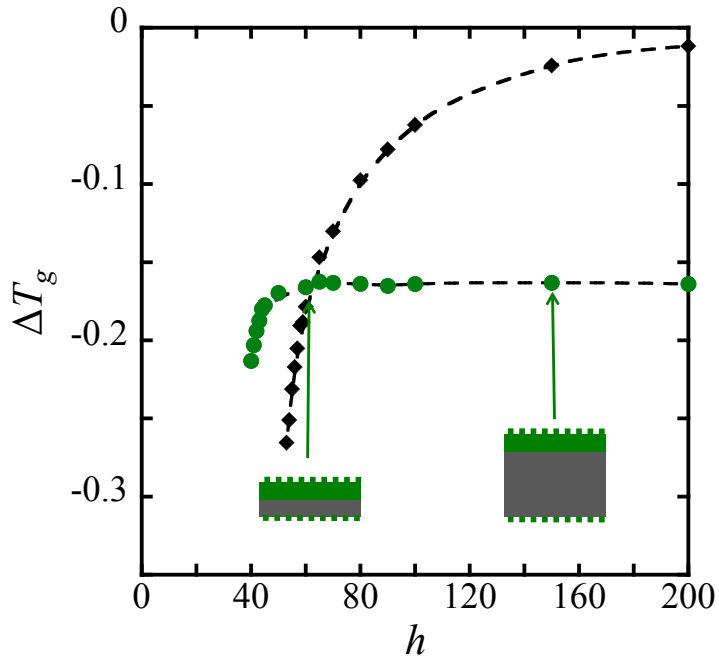


Figure 7: Deviation in local glass transition temperature of free surface reporting layers (green points) from the bulk, $\Delta T_g = T_g - T_{g,\text{bulk}}$, for films of thickness h (in lattice units) with $k = k' = 0.4$. Free-standing film-average results with $k = k' = 0.4$ (black diamonds) are also shown for comparison. Dashed lines are guides to the eye. Inset illustrations show examples of reporting layer thickness (green region) relative to the under-layer thickness (grey region) for 60 and 150 layer thick films.

The surface reporting layer results (green points) of Figure 7 show two regions. In films for which the total thickness ranged from ~50 to 200 lattice layers the ΔT_g is constant at -0.17; once the under-layer is more than about 20 lattice layers thick, adding additional under-layer does not affect the free surface experience. In contrast, over this range of total film thicknesses the *film*-average ΔT_g (black diamonds) varied by an order of magnitude, shifting from approximately -0.01 to -0.20 as the net film diminished in thickness. These results suggest that the mobility local to the free surface reporting layers is not enhanced by the presence of the other free surface in free-standing films greater than 50 lattice layers.

Turning to the results for very thin films (< 50 layers), it is now clear that the negative shift in T_g for free surface reporting layers, alone, increases as the net film thickness decreases. This is the same qualitative behavior as that reported by Kim and Torkelson²⁸ for free-standing PS films. As noted above, they suggested that below a characteristic film thickness, the local T_g of a reporting layer near one free surface is perturbed by the presence of the other free surface located tens of nanometers away.²⁸ Our results support this conclusion, wherein we find that mobility propagating into a film from one free surface enhances the local mobility of reporting layers located at the other free surface in ultrathin free-standing films.

6. Sandwiched reporting layers

Next we direct our focus to the local T_g of reporting layers that are “sandwiched” in a free-standing film, i.e. located at the film’s interior between two “bread” layers. In this case, as the net film thickness increases, the thicknesses of the bread layers on both sides of the reporting layers grow. Equivalently, the distance between the reporting layers and the free surfaces increases as the total film thickness increases. Our approach is analogous to experimental studies^{19,28-30} in which the local glass transition temperature of regions within a film slab located at varying distances from the free surface(s), were probed. For free-standing PS films,²⁸ it was reported that $\Delta T_g = 0$ for a 14 nm PS-pyrene reporting layer sandwiched by two 500 nm unlabeled PS “bread” layers, however, when the thickness of each of the surrounding layers was reduced to 21 nm, the reporting layer

T_g was considerably suppressed, such that $\Delta T_g = -38$ K. Unlike the free surface reporting layers, where ΔT_g was found experimentally to be constant down to a characteristic total film thickness of ~ 50 nm, these results suggest that ΔT_g for sandwiched reporting layers is dependent on the total film thickness, since that determines how close the reporting layer lies relative to the free surfaces.

Once again, the LM model allows us to set up a simulation that models the experimental configuration. Our results, shown in Figure 8, illustrate what we observe for the deviation of the sandwiched reporting layer's glass transition temperature from that of the analogous bulk sample, ΔT_g , as a function of total film thickness, h . Again, we used a reporting layer that was 30 lattice layers thick; for example, for a total film thickness of 90 layers the reporting slice is comprised of layers 31 – 60. Here we make use of results described earlier in the paper that allowed us to optimize the mobility depth, thus we chose $k = k' = 0.10$ in order to optimize the propagation of mobility from the free surfaces into the film interior where the reporting layers are located.

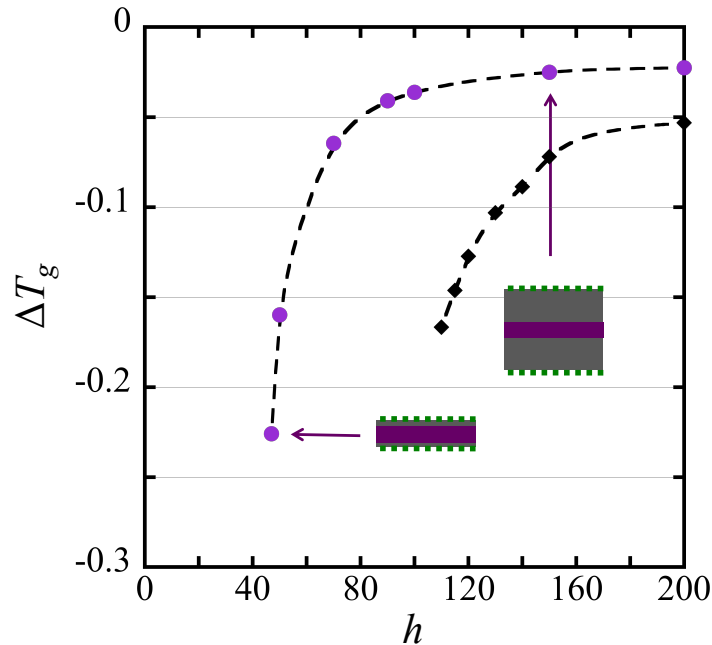


Figure 8: Deviation in local glass transition temperature of sandwiched reporting layers (purple points) from the bulk, $\Delta T_g = T_g - T_{g,\text{bulk}}$, for films of thickness h (in lattice units) with $k = k' = 0.1$. Free-standing film-average results with $k = k' = 0.1$ (black diamonds) are also shown for comparison. Dashed lines are guides to the eye. Inset illustrations show examples of reporting

layer thickness (purple region) relative to the “bread” layer thicknesses (grey regions) for 47 and 150 layer thick films.

The results of Figure 8, all of which are for $k = k' = 0.10$, show that the local T_g of sandwiched reporting layers (purple points) is dependent on the thickness of the “bread” slices, since that, combined with the mobile layer depth, controls the extent of the local glass transition temperature suppression. In thick films, such that $h = 90 - 200$ layers, ΔT_g of the sandwiched reporting layers is relatively constant and approximately equal to -0.025, which means that T_g is effectively that of the bulk. In these cases, the thicknesses of the bread slices exceed the mobile layer depth, which screens the buried layers from the enhanced mobility near the free surfaces.

Comparing the sandwiched reporting layer ΔT_g values with the *total* film-average results (black diamonds) over roughly the same total film thickness range ($h = 90 - 200$ layers), indicates that the film-average T_g is suppressed to a greater extent than the local T_g of a sandwiched reporting layer. For example, the film-average ΔT_g value of a 110 layer thick free-standing film is equal to -0.166, while the ΔT_g value of a sandwiched reporting layer located in the interior of a 110 layer thick film is approximately equal to -0.025. A physical interpretation of these results is that the *interior* of a free-standing film glassifies at a higher temperature than the *overall* film. Glassification occurs at a lower temperature for the overall film because the film-average T_g value is influenced by the regions of enhanced mobility near the free surfaces. Below the bulk T_g , these regions can be sufficiently mobile such that the *overall film average* is melt-like, whereas the film interior is *glassy*. For example, see the $T < T_{g,\text{bulk}}$ mobility profile (blue points) plotted in Figure 5a.

For thinner films, i.e. free-standing films less than ~ 110 layers in total thickness, the overall film will not turn completely glassy, however, its interior region will *locally* glassify down to an overall film thickness of 47 layers. The glassy interior region, as described above, is sandwiched between bread slices that are melt-like. In these very thin films ($h < 90$ overall) the local T_g of the sandwiched reporting layers is notably suppressed from that of the bulk due to the greater propagation of mobility into the

interior. The results presented here agree well qualitatively with the experimental results described above.

7. Conclusions

Using the LM model, we have studied mobility and its temperature dependence in freestanding polymer films under a variety of conditions and compared our results, where possible, with analogous experimental data reported for polymer films. Free surfaces act as sources (and sinks) of mobility in our model, enhancing the likelihood of local motion, relative to that in the film interior. We can control the extent of the mobile layer depth as a function of temperature by tuning the model parameters that control the probability that a site will go dormant (k) or become mobile (k'), the latter event further depending upon an ‘assist’ from a neighboring mobile site. We interpret these parameters as representing intrinsic properties of a fluid, a notion that is supported by comparing some of our simulation results with recent experimental data^{5-8,10-12,13,17} on mobile layer depths in a series of glassy polymeric films. Although our characterization of the mobile layer depth reflects the region of a film where the steady state fraction of mobility is enhanced, we observe some of the same qualitative features of experimental measurements which probe the mobile layer thickness via the local dynamics. For example, results reported by Paeng and Ediger, which showed the growth of the mobile layer as the temperature of the film approaches its bulk T_g and the chemical-structure-dependence of the mobile layer thickness,⁶ which we presume is linked to our model parameters k and k' .

Given that the LM model defines the free surface boundary via a permanently mobile interfacial layer, the criterion of zero mobility that was used in LM studies of bulk systems cannot be applied here. Instead, we define the glass transition temperature as that for which the long-time average fraction of mobility is below 0.1, which is roughly equal to the inverse coordination number (which is 8). This translates into a criterion that at the glass transition an average site has fewer than one mobile neighbor.

We determined film-average glass transition temperatures for freestanding films having a range of thicknesses, and found the film T_g to be suppressed relative to that of

the bulk, such that the effect increases significantly as the film becomes thinner. In connecting with experimental results^{4,19} on PS and PMMA, where the techniques used were sensitive to film density, we are able to deduce a semi-quantitative mapping between 1 lattice layer of a simulated film and approximately 1 nm of a real film. Also in agreement with experiment,⁶¹ we show that the degree of T_g suppression is approximately equal for a free-standing film of thickness h and that of a substrate supported film of thickness $h/2$. As experimental data continue to accumulate, it will be of interest to characterize how T_g reductions are related to both the model parameters k and k' , and chemical/structural differences between materials.

We also probed the effect on T_g of stacking a set of ultrathin free-standing films, in order to make a connection with experimental results showing that when stacked free-standing films are assembled in their glassy state the overall sample melts at a T_g comparable to that of a supported film^{43,45,47,48} or between that of a supported and free-standing film⁴⁶. In our model we simulate the stacked film boundaries by setting the composition at each film interface to be that for the film below its T_g , which means the interfacial mobility is reduced relative to that of a free surface, but greater than that near a substrate. In agreement with experiment, we find that our stacked films melt at a temperature between that of a free and a supported film of analogous thickness. Furthermore, we find that annealing reverses the effect of stacking; i.e., a stacked film that has been annealed glassifies at its bulk T_g , which is also consistent with experimental measurements^{43,45-48}.

Finally, in addition to the film-average T_g studies, we probed the *local* T_g values for a subset of layers in a freestanding film. In particular, we performed local averaging over a set of ‘reporting layers’ located near the free surface and in the film interior, following a procedure similar to that of experimental studies,^{19,28-30} which utilized fluorescence labeled molecules to probe the local density. In the case of free surface reporting layers, we observed that for a reporting thickness of 30 lattice layers near one free surface, the LM results for the T_g suppression was constant down to an overall film thickness of approximately 50 layers. Below this characteristic film thickness, the

reporting layers experienced enhanced mobility propagating from the film’s second free surface, resulting in a significant further decrease in T_g . For reporting layers located at the film’s interior, i.e. “sandwiched” reporting layers, we observed that as the thicknesses of the “bread” layers on either side of the reporting layers grew, the T_g of the interior reporting layers approached that of the bulk. As the surrounding ‘bread layer’ thickness decreased, mobility propagating from the free surfaces extended into the interior reporting layers, resulting in local T_g suppression. In both the free surface and sandwiched reporting layer cases, the change in reporting layer T_g with decreasing film thickness is qualitatively consistent with Kim and Torkelson’s experimental T_g measurements on reporting layers in free-standing PS films²⁸.

We expect that the approach presented here for single layer films could be adapted in order to consider bilayer systems, where each layer comprises a chemically distinct species; e.g., a polystyrene film supported by liquid glycerol^{65,66}. Bilayer films in which the T_g values of the layers differ significantly are of particular interest. Notable work on these systems, such as that of Roth and coworkers^{15,20,29,30} and Lang et al.,³² showed that the presence of an interface between a low T_g (rubbery) and high T_g (glassy) material perturbs the local and film-average physical properties. This would build on previous work,³¹ wherein the LM model predicted that mobility propagates furthest into the less mobile (glassier) region of a *bulk*-like bilayer system. Recent experimental results reported by Baglay and Roth³⁰ on glassy (PS)/rubbery (poly(n-butylmethacrylate)) (PnBMA) bilayer films support this prediction. To this point, we have not applied the LM model to simulate a *film* configuration that consists of two regions with distinct local mobilities, however, this is a potential area for future work.

Acknowledgements

We acknowledge financial support from NSF DMR-1403757 to JEGL, NSF DMR-1507980 to STM, and Graduate Assistance in Areas of National Need (GAANN) to JD. We also thank Nicholas B. Tito for useful discussions.

References

1. Dalnoki-Veress, K.; Forrest, J. A.; Murray, C.; Gigault, C.; Dutcher, J. R. Molecular weight dependence of reductions in the glass transition temperature of thin, freely standing polymer films. *Physical Review E* **2001**, *63*, 031801.
2. Kim, S.; Roth, C. B.; Torkelson, J. M. Effect of Nanoscale Confinement on the Glass Transition Temperature of Free-Standing Polymer Films: Novel, Self-Referencing Fluorescence Method. *Journal of Polymer Science Part B-Polymer Physics* **2008**, *46*, 2754-2764.
3. Mattsson, J.; Forrest, J. A.; Borjesson, L. Quantifying glass transition behavior in ultrathin free-standing polymer films. *Physical Review E* **2000**, *62*, 5187-5200.
4. Keddie, J. L.; Jones, R. A. L.; Cory, R. A. Size-Dependent Depression of the Glass-Transition Temperature in Polymer-Films. *Europhys. Lett.* **1994**, *27*, 59-64.
5. Ediger, M. D.; Forrest, J. A. Dynamics near Free Surfaces and the Glass Transition in Thin Polymer Films: A View to the Future. *Macromolecules* **2014**, *47*, 471-478.
6. Paeng, K.; Ediger, M. D. Molecular Motion in Free-Standing Thin Films of Poly(methyl methacrylate), Poly(4-tert-butylstyrene), Poly(alpha-methylstyrene), and Poly(2-vinylpyridine). *Macromolecules* **2011**, *44*, 7034-7042.
7. Paeng, K.; Swallen, S. F.; Ediger, M. D. Direct Measurement of Molecular Motion in Freestanding Polystyrene Thin Films. *J. Am. Chem. Soc.* **2011**, *133*, 8444-8447.
8. Paeng, K.; Richert, R.; Ediger, M. D. Molecular mobility in supported thin films of polystyrene, poly(methyl methacrylate), and poly(2-vinyl pyridine) probed by dye reorientation. *Soft Matter* **2012**, *8*, 819-826.
9. Baeumchen, O.; McGraw, J. D.; Forrest, J. A.; Dalnoki-Veress, K. Reduced Glass Transition Temperatures in Thin Polymer Films: Surface Effect or Artifact? *Phys. Rev. Lett.* **2012**, *109*, 055701.
10. Qi, D.; Fakhraai, Z.; Forrest, J. A. Substrate and chain size dependence of near surface dynamics of glassy polymers. *Phys. Rev. Lett.* **2008**, *101*, 096101.
11. Qi, D.; Ilton, M.; Forrest, J. A. Measuring surface and bulk relaxation in glassy polymers. *European Physical Journal E* **2011**, *34*, 56.
12. Fakhraai, Z.; Forrest, J. A. Measuring the surface dynamics of glassy polymers. *Science* **2008**, *319*, 600-604.

13. Zuo, B.; Liu, Y.; Wang, L.; Zhu, Y.; Wang, Y.; Wang, X. Depth profile of the segmental dynamics at a poly(methyl methacrylate) film surface. *Soft Matter* **2013**, *9*, 9376-9384.
14. Meyers, G. F.; Dekoven, B. M.; Seitz, J. T. Is the Molecular-Surface of Polystyrene really Glassy. *Langmuir* **1992**, *8*, 2330-2335.
15. Rauscher, P. M.; Pye, J. E.; Baglay, R. R.; Roth, C. B. Effect of Adjacent Rubbery Layers on the Physical Aging of Glassy Polymers. *Macromolecules* **2013**, *46*, 9806-9817.
16. Frenken, J. W. M.; Vanderveen, J. F. Observation of Surface Melting. *Phys. Rev. Lett.* **1985**, *54*, 134-137.
17. Yang, Z.; Fujii, Y.; Lee, F. K.; Lam, C.; Tsui, O. K. C. Glass Transition Dynamics and Surface Layer Mobility in Unentangled Polystyrene Films. *Science* **2010**, *328*, 1676-1679.
18. Lan, T.; Torkelson, J. M. Methacrylate-based polymer films useful in lithographic applications exhibit different glass transition temperature-confinement effects at high and low molecular weight. *Polymer* **2014**, *55*, 1249-1258.
19. Ellison, C. J.; Torkelson, J. M. The distribution of glass-transition temperatures in nanoscopically confined glass formers. *Nature Materials* **2003**, *2*, 695-700.
20. Roth, C. B.; McNerny, K. L.; Jager, W. F.; Torkelson, J. M. Eliminating the enhanced mobility at the free surface of polystyrene: Fluorescence studies of the glass transition temperature in thin bilayer films of immiscible polymers. *Macromolecules* **2007**, *40*, 2568-2574.
21. Baschnagel, J.; Varnik, F. Computer simulations of supercooled polymer melts in the bulk and in-confined geometry. *Journal of Physics-Condensed Matter* **2005**, *17*, R851-R953.
22. Jain, T. S.; de Pablo, J. J. Investigation of transition states in bulk and freestanding film polymer glasses. *Phys. Rev. Lett.* **2004**, *92*, 155505.
23. Shavit, A.; Riggelman, R. A. Influence of Backbone Rigidity on Nanoscale Confinement Effects in Model Glass-Forming Polymers. *Macromolecules* **2013**, *46*, 5044-5052.

24. Mirigian, S.; Schweizer, K. S. Communication: Slow relaxation, spatial mobility gradients, and vitrification in confined films. *J. Chem. Phys.* **2014**, *141*, 161103.

25. Ye, C.; Wiener, C. G.; Tyagi, M.; Uhrig, D.; Orski, S. V.; Soles, C. L.; Vogt, B. D.; Simmons, D. S. Understanding the Decreased Segmental Dynamics of Supported Thin Polymer Films Reported by Incoherent Neutron Scattering. *Macromolecules* **2015**, *48*, 801-808.

26. Xia, W.; Mishra, S.; Keten, S. Substrate vs. free surface: Competing effects on the glass transition of polymer thin films. *Polymer* **2013**, *54*, 5942-5951.

27. Salez, T.; Salez, J.; Dalnoki-Veress, K.; Raphael, E.; Forrest, J. A. Cooperative strings and glassy interfaces. *Proc. Natl. Acad. Sci. U. S. A.* **2015**, *112*, 8227-8231.

28. Kim, S.; Torkelson, J. M. Distribution of Glass Transition Temperatures in Free-Standing, Nanoconfined Polystyrene Films: A Test of de Gennes' Sliding Motion Mechanism. *Macromolecules* **2011**, *44*, 4546-4553.

29. Roth, C. B.; Torkelson, J. M. Selectively probing the glass transition temperature in multilayer polymer films: Equivalence of block copolymers and multilayer films of different homopolymers. *Macromolecules* **2007**, *40*, 3328-3336.

30. Baglay, R. R.; Roth, C. B. Communication: Experimentally determined profile of local glass transition temperature across a glassy-rubbery polymer interface with a T_g difference of 80 K. *J. Chem. Phys.* **2015**, *143*, 111101.

31. Tito, N. B.; Lipson, J. E. G.; Milner, S. T. Lattice model of mobility at interfaces: free surfaces, substrates, and bilayers. *Soft Matter* **2013**, *9*, 9403-9413.

32. Lang, R. J.; Merling, W. L.; Simmons, D. S. Combined Dependence of Nanoconfined T_g on Interfacial Energy and Softness of Confinement. *Acs Macro Letters* **2014**, *3*, 758-762.

33. Keddie, J. L.; Jones, R. A. L.; Cory, R. A. Interface and Surface Effects on the Glass-Transition Temperature in Thin Polymer-Films. *Faraday Discuss.* **1994**, *98*, 219-230.

34. Fryer, D. S.; Nealey, P. F.; de Pablo, J. J. Thermal probe measurements of the glass transition temperature for ultrathin polymer films as a function of thickness. *Macromolecules* **2000**, *33*, 6439-6447.

35. Grohens, Y.; Hamon, L.; Reiter, G.; Soldera, A.; Holl, Y. Some relevant parameters affecting the glass transition of supported ultra-thin polymer films. *European Physical Journal E* **2002**, *8*, 217-224.

36. Sanders, D. E.; Smith, Z. P.; Guo, R.; Robeson, L. M.; McGrath, J. E.; Paul, D. R.; Freeman, B. D. Energy-efficient polymeric gas separation membranes for a sustainable future: A review. *Polymer* **2013**, *54*, 4729-4761.

37. Baker, R. W.; Low, B. T. Gas Separation Membrane Materials: A Perspective. *Macromolecules* **2014**, *47*, 6999-7013.

38. Tito, N. B.; Lipson, J. E. G.; Milner, S. T. Lattice model of dynamic heterogeneity and kinetic arrest in glass-forming liquids. *Soft Matter* **2013**, *9*, 3173-3180.

39. Karim, T. B.; McKenna, G. B. Unusual Surface Mechanical Properties of Poly(alpha-methylstyrene): Surface Softening and Stiffening at Different Temperatures. *Macromolecules* **2012**, *45*, 9697-9706.

40. Yoon, H.; McKenna, G. B. Substrate Effects on Glass Transition and Free Surface Viscoelasticity of Ultrathin Polystyrene Films. *Macromolecules* **2014**, *47*, 8808-8818.

41. Chen, F.; Lam, C.; Tsui, O. K. C. The Surface Mobility of Glasses. *Science* **2014**, *343*, 975-976.

42. Glor, E. C.; Fakhraai, Z. Facilitation of interfacial dynamics in entangled polymer films. *J. Chem. Phys.* **2014**, *141*, 194505.

43. Koh, Y. P.; McKenna, G. B.; Simon, S. L. Calorimetric glass transition temperature and absolute heat capacity of polystyrene ultrathin films. *Journal of Polymer Science Part B-Polymer Physics* **2006**, *44*, 3518-3527.

44. Koh, Y. P.; Simon, S. L. Structural Relaxation of Stacked Ultrathin Polystyrene Films. *Journal of Polymer Science Part B-Polymer Physics* **2008**, *46*, 2741-2753.

45. Hayashi, T.; Fukao, K. Segmental and local dynamics of stacked thin films of poly(methyl methacrylate). *Physical Review E* **2014**, *89*, 022602.

46. Fukao, K.; Oda, Y.; Nakamura, K.; Tahara, D. Glass transition and dynamics of single and stacked thin films of poly(2-chlorostyrene). *European Physical Journal-Special Topics* **2010**, *189*, 165-171.

47. Fukao, K.; Terasawa, T.; Oda, Y.; Nakamura, K.; Tahara, D. Glass transition dynamics of stacked thin polymer films. *Physical Review E* **2011**, *84*, 041808.

48. Lai, C.; Ayyer, R.; Hiltner, A.; Baer, E. Effect of confinement on the relaxation behavior of poly(ethylene oxide). *Polymer* **2010**, *51*, 1820-1829.

49. de Gennes, P. G. Glass transitions in thin polymer films. *European Physical Journal E* **2000**, *2*, 201-203.

50. Priestley, R. D.; Cangialosi, D.; Napolitano, S. On the equivalence between the thermodynamic and dynamic measurements of the glass transition in confined polymers. *J. Non Cryst. Solids* **2015**, *407*, 288-295.

51. Glor, E. C.; Composto, R. J.; Fakhraai, Z. Glass Transition Dynamics and Fragility of Ultrathin Miscible Polymer Blend Films. *Macromolecules* **2015**, *48*, 6682-6689.

52. Mckenna, G. B. Dilatometric Evidence for the Apparent Decoupling of Glassy Structure from the Mechanical-Stress Field. *J. Non Cryst. Solids* **1994**, *172*, 756-764.

53. Simon, S. L.; Sobieski, J. W.; Plazek, D. J. Volume and enthalpy recovery of polystyrene. *Polymer* **2001**, *42*, 2555-2567.

54. Santore, M. M.; Duran, R. S.; Mckenna, G. B. Volume Recovery in Epoxy Glasses Subjected to Torsional Deformations - the Question of Rejuvenation. *Polymer* **1991**, *32*, 2377-2381.

55. Delaye, J. M.; Limoge, Y. Simulation of Vacancies in a Lennard-Jones Glass. *J. Non Cryst. Solids* **1993**, *156*, 982-985.

56. Donati, C.; Glotzer, S. C.; Poole, P. H.; Kob, W.; Plimpton, S. J. Spatial correlations of mobility and immobility in a glass-forming Lennard-Jones liquid. *Physical Review E* **1999**, *60*, 3107-3119.

57. Fredrickson, G. H.; Andersen, H. C. Facilitated Kinetic Ising-Models and the Glass-Transition. *J. Chem. Phys.* **1985**, *83*, 5822-5831.

58. Tito, N. B.; Milner, S. T.; Lipson, J. E. G. Enhanced diffusion and mobile fronts in a simple lattice model of glass-forming liquids. *Soft Matter* **2015**, *11*, 7792-7801.

59. Lipson, J. E. G.; Milner, S. T. Percolation model of interfacial effects in polymeric glasses. *European Physical Journal B* **2009**, *72*, 133-137.

60. Pye, J. E.; Roth, C. B. Above, Below, and In-Between the Two Glass Transitions of Ultrathin Free-Standing Polystyrene Films: Thermal Expansion Coefficient and Physical Aging. *Journal of Polymer Science Part B-Polymer Physics* **2015**, *53*, 64-75.

61. Forrest, J. A.; Mattsson, J. Reductions of the glass transition temperature in thin polymer films: Probing the length scale of cooperative dynamics. *Physical Review E* **2000**, *61*, R53-R56.
62. Roth, C. B.; Pound, A.; Kamp, S. W.; Murray, C. A.; Dutcher, J. R. Molecular-weight dependence of the glass transition temperature of freely-standing poly(methyl methacrylate) films. *European Physical Journal E* **2006**, *20*, 441-448.
63. O'Connell, P. A.; Wang, J.; Ishola, T. A.; McKenna, G. B. Exceptional Property Changes in Ultrathin Films of Polycarbonate: Glass Temperature, Rubbery Stiffening, and Flow. *Macromolecules* **2012**, *45*, 2453-2459.
64. Li, X.; McKenna, G. B. Ultrathin Polymer Films: Rubbery Stiffening, Fragility, and T-g Reduction. *Macromolecules* **2015**, *48*, 6329-6336.
65. Bodiguel, H.; Fretigny, C. Viscoelastic dewetting of a polymer film on a liquid substrate. *European Physical Journal E* **2006**, *19*, 185-193.
66. Wang, J.; McKenna, G. B. Viscoelastic and Glass Transition Properties of Ultrathin Polystyrene Films by Dewetting from Liquid Glycerol. *Macromolecules* **2013**, *46*, 2485-2495.

for Table of Contents use only

Simulating Local T_g Reporting Layers in Glassy Thin Films

Jeffrey DeFelice, Scott T. Milner, and Jane E. G. Lipson

